



Reaction and complex formation between OH radical and acetone

Gábor Vasvári, István Szilágyi, Ákos Bencsura, Sándor Dóbe', Tibor Be'rces, Eric Henon, Sebastien Canneaux, Fre'de'ric Bohr

► To cite this version:

Gábor Vasvári, István Szilágyi, Ákos Bencsura, Sándor Dóbe', Tibor Be'rces, et al.. Reaction and complex formation between OH radical and acetone. *Physical Chemistry Chemical Physics*, 2001, 3 (4), pp.551-555. 10.1039/B009601F . hal-03377098

HAL Id: hal-03377098

<https://hal.univ-reims.fr/hal-03377098>

Submitted on 14 Oct 2021

HAL is a multi-disciplinary open access archive for the deposit and dissemination of scientific research documents, whether they are published or not. The documents may come from teaching and research institutions in France or abroad, or from public or private research centers.

L'archive ouverte pluridisciplinaire **HAL**, est destinée au dépôt et à la diffusion de documents scientifiques de niveau recherche, publiés ou non, émanant des établissements d'enseignement et de recherche français ou étrangers, des laboratoires publics ou privés.

Reaction and complex formation between OH radical and acetone

Gábor Vasvári,^a István Szilágyi,^a Ákos Bencsura,^a Sándor Dóbé,^{*a} Tibor Bérces,^a Eric Henon,^{*b} Sebastien Canneaux^b and Frédéric Bohr^b

^a Chemical Research Center, Hungarian Academy of Sciences, Pusztaszeri u. 59-67, H-1025 Budapest, Hungary. E-mail: dobe@chemres.hu

^b Laboratoire de Chimie-Physique, GSMA, URA D1434, Faculté des Sciences de Reims, Moulin de la House, BP 1039, 51687, Cedex 2, France

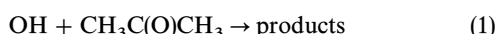
Received 30th November 2000, Accepted 14th December 2000

First published as an Advance Article on the web 12th January 2001

Kinetics and mechanism of the reaction of OH with CH₃C(O)CH₃ have been studied by discharge-flow experiments and CCSD(T) quantum chemical computations. In the experiments, the rate coefficient for the overall reaction, OH + CH₃C(O)CH₃ → products (1), and the branching ratio for the specific reaction channel OH + CH₃C(O)CH₃ → CH₂C(O)CH₃ + H₂O (1a) have been determined to be $k_1 = (1.04 \pm 0.03) \times 10^{11} \text{ cm}^3 \text{ mol}^{-1} \text{ s}^{-1}$ and $\Gamma_{1a} = k_{1a}/k_1 = 0.50 \pm 0.04$, respectively ($T = 298 \text{ K}$). Two different reaction pathways have been characterized by *ab initio* calculations. Both H atom abstraction and OH addition to the C=O group have been found to occur through hydrogen bonded OH...CH₃C(O)CH₃ complexes. Most of our results support recent findings (M. Wollenhaupt, S. A. Carl, A. Horowitz and J. N. Crowley, *J. Phys. Chem. A*, 2000, **104**, 2695; M. Wollenhaupt and J. N. Crowley, *J. Phys. Chem. A*, 2000, **104**, 6429) but contradictions remain concerning the mechanism of this atmospherically important reaction.

Recent field measurements have revealed that acetone is present in surprisingly high concentration in the atmosphere.¹ It has been shown^{1a–3} that atmospheric degradation of acetone can be the dominant source of HO_x (OH and HO₂) radicals in the upper troposphere resulting in increased ozone production.⁴ Sources of acetone in the atmosphere include oxidation of non-methane hydrocarbons, biogenic and anthropogenic emissions and biomass burning.⁵ Major sinks are photodecomposition⁶ (the main loss process) and reaction with OH.⁷

Kinetic studies of the reaction of OH radical with acetone have been reviewed.^{8,9} Very recently, numerous new investigations have been performed and reported in close succession.^{7,10–12} In most of the kinetic experiments, the overall reaction (1) was studied at and above room temperature where the rate coefficients determined were found to obey Arrhenius law.^{8,9}



The reaction was assumed to proceed *via* H-atom abstraction, (1a), producing acetyl radical, CH₂C(O)CH₃:



Wollenhaupt *et al.*⁷ was the first who extended the temperature-range of the investigations down to that typical of the upper troposphere ($T \approx 200 \text{ K}$). The authors observed strong non-Arrhenius behaviour for the overall reaction of OH with acetone. The rate coefficient, k_1 , was found to decrease with decreasing temperature, first fast, but only slowly below room temperature, reaching a minimum at around 240 K, then increasing again slightly below this temperature. The temperature dependence was explained⁷ by the existence of two reaction routes. Accordingly, the reaction proceeds *via* H atom abstraction (1a) at higher temperatures, while below room temperature methyl elimination (1b) dominates:



In a subsequent publication, Wollenhaupt and Crowley¹¹ presented experimental evidence for the formation of CH₃ in the reaction of OH with acetone. Based on the temperature dependence of k_1 and the measured CH₃ yields, reaction (1b) was proposed^{7,11} to occur *via* an addition–elimination mechanism, where addition of OH to the carbonyl C atom is followed by elimination of CH₃ from the vibrationally excited addition radical (CH₃C(OH)(O)CH₃)*.

The very recent experimental studies^{7,11,12} clearly indicate a complex mechanism for the reaction of OH radical with acetone. However, despite a wealth of information supplied by these new studies, important features of the reaction are not yet known. Such are, for example, the effect of pressure on the reaction, the branching ratio for the H abstraction channel and the question of how the assumed reaction mechanism conforms to theoretical models.

In this paper we present experimental results obtained at room temperature for k_1 and the branching ratio $\Gamma_{1a} = k_{1a}/k_1$, and report parts of the results from *ab initio* molecular orbital computations.¹³

The discharge-flow (DF) method was applied to carry out the experiments. Two kinetic set-ups were used. One of them served for the determination of the rate coefficient of the overall reaction using resonance fluorescence monitoring of the OH radical (DF/RF). The other apparatus was equipped with laser induced fluorescence detection (DF/LIF) to determine the reaction branching ratio. OH radicals were generated inside of a moveable injector by reacting H atoms with NO₂ and F atoms with H₂O in the DF/RF and DF/LIF experiments, respectively. OH and acetyl (1-methylvinoyl) radicals were detected in the DF/LIF experiments following excitation in the (1,0) band of the A–X transition at 282 nm¹⁴ and in the electronic transition at 340 nm,¹⁵ respectively. Laser radiation was provided by a Nd:YAG pumped frequency-doubled tunable dye laser. Helium (Messer-Griesheim, 99.9990%) was the carrier gas. High purity acetone (Aldrich, 99.9+%) was used in the experiments which was degassed by repeated freeze–pump–thaw cycles prior to use. The initial concentration of OH was $[\text{OH}]_0 \leq 7 \times 10^{-13} \text{ mol}$

cm^{-3} ; acetone was present in large excess ($[\text{CH}_3\text{C}(\text{O})\text{CH}_3] \gg [\text{OH}]_0$).

The usual pseudo-first-order experiments and evaluation procedure were used to determine the rate coefficient of the overall reaction (1). Representative pseudo-first-order plots are presented in Fig. 1. Experimental conditions and results are summarized in Table 1. Most of the experiments were carried out by the DF/RF method resulting in the recommended rate coefficient of

$$k_1(298 \text{ K}) = (1.04 \pm 0.03) \times 10^{11} \text{ cm}^3 \text{ mol}^{-1} \text{ s}^{-1},$$

with 1σ statistical error quoted. In a few experiments, the DF/LIF method with different OH source was applied giving essentially the same result (see Table 1). Our rate coefficient value agrees well with the recent IUPAC recommendation,⁹ $k_1(298 \text{ K}) = (1.14 \pm 0.09) \times 10^{11} \text{ cm}^3 \text{ mol}^{-1} \text{ s}^{-1}$, and is in excellent agreement with the very recent determination by Wollenhaupt *et al.*⁷ which is $k_1(298 \text{ K}) = (1.04 \pm 0.05) \times 10^{11} \text{ cm}^3 \text{ mol}^{-1} \text{ s}^{-1}$. Wollenhaupt *et al.*⁷ applied the laser flash photolysis method combined with laser induced fluorescence detection of OH radicals at 27, 67, and 133 mbar of Ar or N_2 bath gas under conditions where probable systematic errors were virtually eliminated. The very good agreement of the rate coefficients gives credit to them, particularly because we used the non-photolytic discharge-flow method while in all previous determinations the OH radicals were produced by UV-photolysis.^{7–12} Our measurements were carried out at low pressures ($P \approx 3$ mbar He). Comparison with published results^{7–12} reveals no systematic variation of k_1 with reaction pressure. This is actually what is anticipated for a direct H atom abstraction reaction. The observation of pressure dependence would have provided strong evidence for the formation

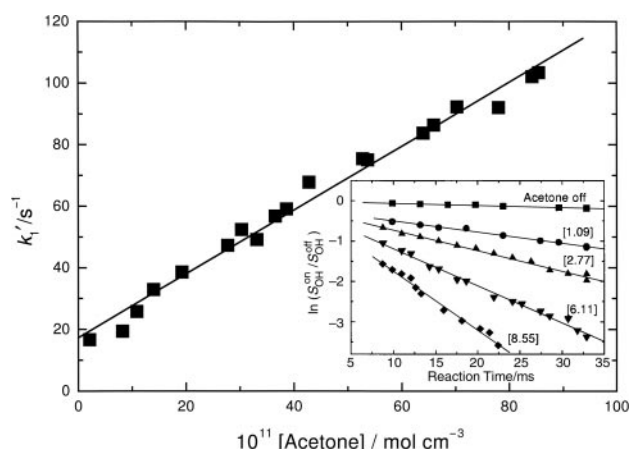


Fig. 1 Plots used for the determination of the rate coefficient for the overall reaction of OH with acetone. The kinetic data plotted were obtained from DF/RF experiments at $T = 298 \text{ K}$. The inset shows representative pseudo-first-order decay plots, where $S_{\text{OH}}^{\text{on}}$ and $S_{\text{OH}}^{\text{off}}$ designate OH resonance fluorescence signal-strengths in the presence and absence of acetone, respectively. The numbers given in square brackets refer to $\text{CH}_3\text{C}(\text{O})\text{CH}_3$ concentrations in $10^{-10} \text{ mol cm}^{-3}$. The slopes of the straight lines of the semilogarithmic decay plots give the pseudo-first-order rate coefficient, k'_1 . The bimolecular rate coefficient, k_1 , is obtained from the plot of $k'_1 = k_1[\text{acetone}] + \text{const}$. The straight lines are linear least-squares fits to the data.

of an energized adduct (an addition radical or radical-molecule complex) that could be stabilized by collisions. Obviously, the reverse statement is not true: the absence of pressure dependence does not exclude the formation of adduct intermediates. That is, the pressure independence observed for k_1 neither proves nor disproves the existence of an addition-elimination mechanism for the reaction of OH with acetone.

In the DF/LIF kinetic experiments, the consumption of OH was accompanied by a parallel build-up of $\text{CH}_2\text{C}(\text{O})\text{CH}_3$, providing evidence for reaction (1a). Representative kinetic curves for OH and $\text{CH}_2\text{C}(\text{O})\text{CH}_3$ are shown in Fig. 2. The branching ratio of reaction (1a) has been determined by computer simulations of the measured concentration *vs.* time profiles¹³ and a comparative method, similar to the one we used in a previous work.¹⁶ Results obtained by the comparative method are presented here. In this case, the reaction of F atom with acetone served as a reference, the acetonyl-yield for which was assumed to be 100%. Experiments were carried out in the following way: F atoms were introduced through the moveable injector into the reactor at a fixed distance (constant reaction time), were mixed up with acetone in high excess ($[\text{CH}_3\text{C}(\text{O})\text{CH}_3] \gg [\text{F}]_0$) to assure complete conversion, and the LIF signal-strengths of acetonyl radicals formed, $S_{\text{CH}_2\text{C}(\text{O})\text{CH}_3}^{(\text{F} + \text{acetone})}$, were recorded. Under the very same conditions, with the exception that fluorine atoms were converted to OH by the reaction with H_2O inside the injector, the LIF signal-strengths of the acetonyl radicals for the studied reaction, $S_{\text{CH}_2\text{C}(\text{O})\text{CH}_3}^{(\text{OH} + \text{acetone})}$, were recorded. The branching ratio for reaction (1a) was obtained from the ratio $S_{\text{CH}_2\text{C}(\text{O})\text{CH}_3}^{(\text{OH} + \text{acetone})} / S_{\text{CH}_2\text{C}(\text{O})\text{CH}_3}^{(\text{F} + \text{acetone})}$. A small correction was made to take into account the different wall-losses of F and OH. Multiple determinations were performed with an approximately 10-fold variation in $[\text{F}]_0$. The average of the results is the recommended branching ratio for

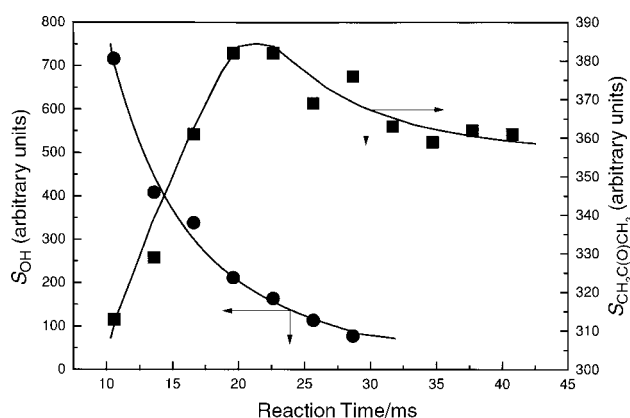


Fig. 2 Consumption of OH and formation of acetonyl in a typical DF/LIF experiment of the OH + $\text{CH}_3\text{C}(\text{O})\text{CH}_3$ reaction. Experimental conditions were as follows: $T = 300 \text{ K}$, $P = 2.83 \text{ mbar}$, $[\text{F}]_0 = [\text{OH}]_0 = 3 \times 10^{-13} \text{ mol cm}^{-3}$, $[\text{H}_2\text{O}] = 7 \times 10^{-12} \text{ mol cm}^{-3}$, $[\text{acetone}] = 9.7 \times 10^{-10} \text{ mol cm}^{-3}$. S_{OH} and $S_{\text{CH}_2\text{C}(\text{O})\text{CH}_3}$ designate the concentration-proportional LIF signal strengths for the OH and acetonyl radicals, respectively. The solid curves were obtained from computer simulations of a multi-reaction mechanism, where the only fitted parameter was the branching ratio of the acetonyl-forming reaction channel, i.e. $\Gamma_{1a} = k_{1a}/k_1$.¹³

Table 1 Experimental conditions and kinetic results for the reaction $\text{OH} + \text{CH}_3\text{C}(\text{O})\text{CH}_3 \rightarrow \text{products}$ (1)^a

Method	OH source	No. of expts.	T/K	P/mbar	$v/\text{cm s}^{-1}$	$10^{11} [\text{CH}_3\text{C}(\text{O})\text{CH}_3]/\text{mol cm}^{-3}$	k_w^b/s^{-1}	k'_1/s^{-1}	$10^{-10} k_1/\text{cm}^3 \text{ mol}^{-1} \text{ s}^{-1}$
DR/RF	H + NO_2	19	298 ± 2	2.63	779	2.10–85.5	9 ± 6^c	17–103	10.4 ± 0.30
DF/LIF	F + H_2O	5	300 ± 2	2.82	345	97.0–160	3 ± 2^d	91–150	9.97 ± 0.65

^a Quoted errors represent 1σ (precision only). ^b Heterogeneous loss of OH radicals. ^c PTFE wall coating. ^d Halocarbon wax wall coating.

the H abstraction reaction channel:

$$\Gamma_{1a} = \frac{k_{1a}}{k_1} = 0.50 \pm 0.04 \quad (T = 298 \text{ K})$$

The assumption that the reference reaction $F + \text{CH}_3\text{C}(\text{O})\text{CH}_3$ proceeds exclusively *via* H-atom abstraction was tested by comparison with the $\text{Cl} + \text{CH}_3\text{C}(\text{O})\text{CH}_3$ reaction in an experimental arrangement similar to that described above (conversion of F to Cl was achieved by the reaction of F with HCl). The average of the ratio of the respective signal-strengths was found to be $S_{\text{CH}_3\text{C}(\text{O})\text{CH}_3}^{(\text{Cl}+\text{acetone})}/S_{\text{CH}_3\text{C}(\text{O})\text{CH}_3}^{(\text{F}+\text{acetone})} = 1.03 \pm 0.07$ which is believed to be a strong indication for practically 100% acetonyl yields in the reactions of acetone with both F and Cl. The branching ratio determined by us for reaction channel (1a) is significantly less than one, indicating that a simple H atom abstraction can not be the only reaction mechanism for the reaction of OH with acetone. This is in line with the findings of Wollenhaupt and Crowley¹¹ who reported the value of

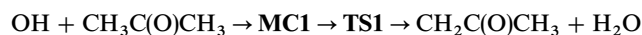
$$\Gamma_{1b} = \frac{k_{1b}}{k_1} = 0.50 \pm 0.15$$

for the $\text{CH}_3 + \text{CH}_3\text{COOH}$ forming channel (1b). Wollenhaupt and Crowley monitored the formation of CH_3 *via* a conversion reaction with NO_2 in the form of CH_3O using LIF detection in laser flash photolysis experiments; Γ_{1b} was obtained by fitting of an assumed reaction mechanism to the measured CH_3O profiles.¹¹ The two branching ratios, determined by Wollenhaupt and Crowley and by us, complement each other, $\Gamma_{1a} + \Gamma_{1b} \approx 1$, which may be taken as an indirect support for their reliability.

Collaterally with the experimental work, we have performed *ab initio* molecular orbital computations to get an insight into the mechanism of the reaction of OH with acetone. Reaction pathways have been explored on the potential energy surface for the hydrogen abstraction reaction and the OH addition to the carbon atom of the C=O group. Both reactions were found to occur through loosely bound $\text{OH} \cdots \text{CH}_3\text{C}(\text{O})\text{CH}_3$ com-

plexes preceding transition states. *Ab initio* calculations were performed using the GAUSSIAN 94 software package.¹⁷ Reactants, complexes, transition-state structures and products were fully optimized using the analytical gradients at the MP2 level of theory,¹⁸ with the 6-31G(d,p) basis set. The minimum energy path (MEP) was examined by the IRC procedure;¹⁹ the transition states were found to connect proper reactants and products. Single-point calculations applying the CCSD(T) method²⁰ with the 6-311G(d,p) basis set were carried out to obtain energy differences for stationary structures. The “frozen-core” approximation was used both in Møller-Plesset and CCSD(T) calculations. Some of the structural features and the zero-point energy corrected relative energies computed for the reaction $\text{OH} + \text{CH}_3\text{C}(\text{O})\text{CH}_3$ are summarized in Fig. 3. Detailed geometries and harmonic vibrational frequencies will be given in a later publication.¹³

Our theoretical investigations have revealed a pathway for the H atom abstraction reaction which can be summarized as



where **MC1** and **TS1** designate hydrogen-brided complex and reaction transition state, respectively. **MC1** was found as local minimum on the potential energy surface with 26.3 kJ mol^{-1} binding energy (D_0) relative to the reactants. It has a six-membered ring-like structure formed by the hydroxy and H(1), C(2), C(1) and O(1) atoms of the acetone molecule (see Fig. 3). The calculations predicted a nearly planar structure for OH approach to the C(2)C(1)C(3) frame of acetone. In a very recent work, Aloisio and Francisco²¹ have found an $\text{OH} \cdots \text{CH}_3\text{C}(\text{O})\text{CH}_3$ complex, very similar to **MC1**, using density functional theory method. Applying the best level of theory [B3LYP/6-31++G(3df,3pd)] the authors reported 19.3 kJ mol^{-1} binding energy. Besides the $\text{OH} \cdots \text{CH}_3\text{C}(\text{O})\text{CH}_3$ complex, no other portion of the potential energy surface was investigated by Aloisio and Francisco.²¹ The structure of **TS1** has a close resemblance to that of **MC1**, the transition state being practically “preformed” by the hydrogen-bonded complex. The computed barrier is 16.7 kJ mol^{-1} above the reactants. Traditionally, hydrogen-transfer reactions, such as

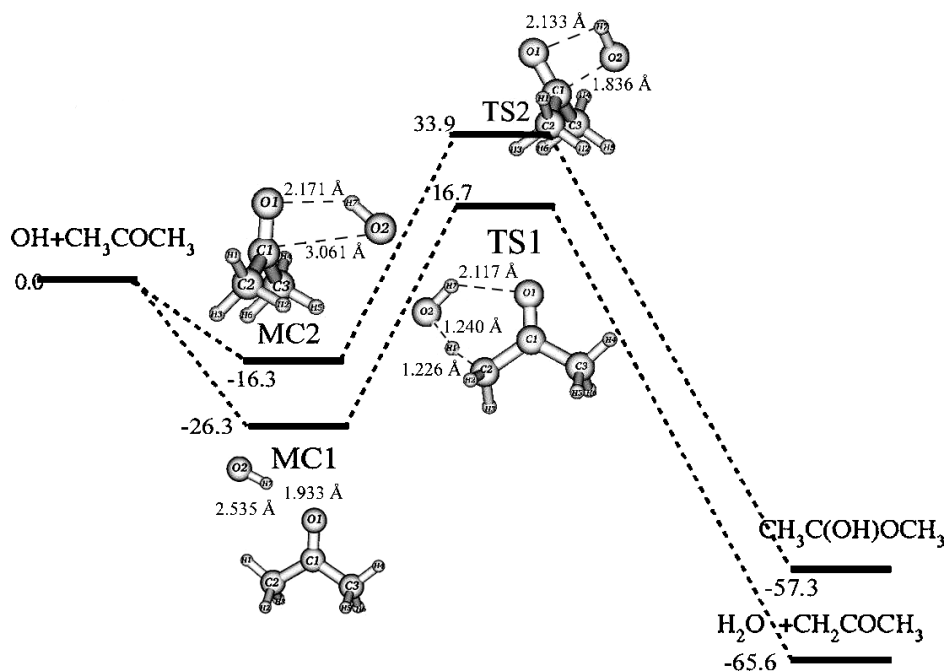
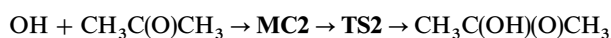


Fig. 3 Schematic molecular structures and energetics for $\text{OH} + \text{CH}_3\text{C}(\text{O})\text{CH}_3$ obtained from *ab initio* computations at the CCSD(T)/6-311G(d,p)//MP2/6-31G(d,p) level of theory. **MC1** and **MC2** designate $\text{OH} \cdots \text{CH}_3\text{C}(\text{O})\text{CH}_3$ complexes formed on along the H atom abstraction reaction path and the C=O addition reaction path, respectively. **TS1** and **TS2** are transition states, the structures of which are similar to those of the respective $\text{OH} \cdots \text{CH}_3\text{C}(\text{O})\text{CH}_3$ complexes, **MC1** and **MC2**. OH-attack takes place approximately in the plane and perpendicularly to the plane defined by the C(2)C(1)C(3) skeleton of the acetone molecule in case of the abstraction reaction and addition reaction, respectively. The energy data are given in kJ mol^{-1} and include zero-point energy corrections.

reaction (1a), have been thought of as direct metathesis reactions with a single barrier and transition state along the reaction coordinate. There are more and more indications, however, from theoretical studies (*e.g.* ref. 22) and also from sophisticated experimental works (*e.g.* ref. 23) that the kinetic and dynamic properties of many of the H atom abstraction reactions are connected to the formation of loose radical-molecule complexes. In certain cases, the direct H atom transfer is "assisted"²⁴ by intermolecular noncovalent bonding interactions. This is what is believed to be the case for reaction (1a) suggested by our theoretical results as well.

In experimental works of the reactions of atoms and free radicals with carbonyl compounds (aldehydes and ketones), the addition to the C=O bond was occasionally suggested to explain the observed product yields, but unambiguous experimental evidence has been scarce (see *e.g.* ref. 25 and references therein). We are aware of only two theoretical studies which dealt with the addition reaction of OH to the carbonyl double bond^{26,27}. In our CCSD(T) computations, addition to the carbon atom of the C=O group was found to occur through a loosely bound complex, **MC2**, with similar structure to that of the transition state, **TS2**, that leads to the formation of the addition radical α -hydroxy-i-propoxy in the reaction:



The incoming OH radical [O(2)H(7)] approaches the C(1) site from a direction nearly perpendicular to the molecular plane containing the C(2)C(1)C(3) skeleton of the acetone molecule (see Fig. 3). In **MC2**, a four-membered ring is formed by the hydroxyl radical and the C(1) and O(1) atoms of the acetone molecule. As in the case of the abstraction complex, the intermolecular hydrogen bond is formed between the hydrogen atom of the OH radical, H(7), and the oxygen atom of the acetone molecule, O(1). The binding energy for **MC2** was calculated to be 16.3 kJ mol⁻¹, that is, the addition complex is less stable by 10 kJ mol⁻¹ than its abstraction counterpart. The four-membered ring structure is preserved in the transition state, **TS2**, but with a much smaller O(2)–C(1) bond distance [O(2)–C(1) = 1.836 Å]. This bond distance is very close to that calculated by Soto and Page²⁶ at the CASSCF(3,3)/DZP level of theory [O(2)–C(1) = 1.834 Å²⁶] in their study of the potential energy surface for addition of OH to the carbon atom of formaldehyde. The barrier height computed for the addition channel is 33.9 kJ mol⁻¹ which agrees favourably with the barrier of 29.2 kJ mol⁻¹ predicted by Soto and Page²⁶ at the MRCI/DZP level for OH addition to formaldehyde. The exit channels on the potential energy surface for CH₃C(OH)(O)CH₃ (*e.g.* CH₃ + CH₃COOH) have not been investigated in the current work. We note, moreover, that addition of OH to the O atom of the carbonyl group is strongly endothermic²⁶ and does not play any role under ambient conditions.

The experimentally measured temperature dependence of k_1 has been described by Wollenhaupt *et al.*⁷ by a double exponential equation:

$$\begin{aligned} k_1(202\text{--}395 \text{ K}) \\ = (5.3 \pm 2.2) \times 10^{12} \exp[(-11.0 \pm 1.4 \text{ kJ mol}^{-1})/RT] \\ + (1.0 \pm 0.5) \times 10^{10} \exp[(3.5 \pm 0.9 \text{ kJ mol}^{-1})/RT] \\ \times \text{cm}^3 \text{ mol}^{-1} \text{ s}^{-1} \end{aligned}$$

attributing the first term to direct H abstraction and the second one to addition. The zero-point energy corrected barrier computed in the current work for the abstraction pathway at the CCSD(T) level of theory is about 6 kJ mol⁻¹ larger (16.7 kJ mol⁻¹) than the experimental activation energy (11.0 kJ mol⁻¹), but this is a reasonable agreement and within the likely uncertainties (the agreement between the *A*-factors is also satisfactory¹³). On the other hand, the high activation

barrier computed for the addition reaction of OH to the carbonyl C=O bond of acetone (33.9 kJ mol⁻¹) is clearly inconsistent with the negative (–3.5 kJ mol⁻¹) experimental activation energy and therefore with the assumption of a fast addition-elimination reaction through the energized (CH₃C(OH)(O)CH₃)* radical that might explain the large k_1 values and high CH₃ yields in the experiments at and below room temperature.^{7,11} Computations at even higher level of theory and with the application of more sophisticated basis sets are not expected to bring down the addition-channel barrier height close to the value of the experimental activation energy. Therefore, given the high CH₃ yields observed experimentally,¹¹ we speculate that there must be a hitherto unexplored mechanism that does not involve the formation of the addition radical CH₃C(OH)(O)CH₃. It is not unreasonable to assume, for example, the occurrence of a concerted mechanism for the reaction of OH radical with acetone that directly leads to CH₃ and CH₃COOH formation *via* a low activation energy process.

Atmospheric implications of our kinetic results are in accordance with recent conclusions.^{7,11,12} The pressure independent rate coefficient measured in the present study supports the view^{7,12} that reaction (1) is a more important sink for acetone in the upper troposphere than it was thought before. On the basis of product studies performed by Wollenhaupt and Crowley¹¹ and in the current work, it appears well established that the branching ratios are ≈ 0.5 for both the CH₃C(O)CH₃ + H₂O (1a) and the CH₃ + CH₃COOH (1b) reaction channels at room temperature. A consistent mechanism is still lacking, however, which would explain the observed product yields and the temperature dependence of k_1 ,^{7,12} and would allow reliable predictions to be made for atmospheric modeling studies. Experimental determination of the temperature dependencies of product yields and a search for further stationary structures on the potential energy surface would be particularly useful in elucidating the mechanism of the reaction of OH with acetone.

Acknowledgements

This work has been supported by the French–Hungarian Intergovernmental Program (contract No. F-8/98) and the German–Hungarian Intergovernmental Program (contract No. D-8/98). The I.D.R.I.S. and C.R.I.H.A.N. computing centers are acknowledged for the CPU time granted. The authors appreciate the assistance of Mr T. Köcher in some of the experiments.

References

- (a) H. B. Singh, M. Kanakidou, P. J. Crutzen and D. J. Jacob, *Nature*, 1995, **378**, 50; (b) F. Arnold, J. Schneider, K. Gollinger, H. Schlager, P. Schulte, D. E. Hage, P. D. Whitefield and P. van Velthoven, *Geophys. Res. Lett.*, 1997, **24**, 57.
- S. A. McKeen, T. Gierczak, J. B. Burkholder, P. O. Wennberg, T. F. Hanisco, E. R. Keim, R.-S. Gao, S. C. Liu, A. R. Ravishankara and D. W. Fahey, *Geophys. Res. Lett.*, 1997, **24**, 3177.
- P. O. Wennberg, T. F. Hanisco, L. Jaeglé, D. J. Jacob, E. J. Hints, E. J. Lanzendorf, J. G. Anderson, R.-S. Gao, E. R. Keim, S. G. Donnelly, L. A. Del Negro, D. W. Fahey, S. A. McKeen, R. J. Salawitch, C. R. Webster, R. D. May, R. L. Herman, M. H. Proffitt, J. J. Margitan, E. L. Atlas, S. M. Schauffler, F. Flocke, C. T. McElroy and T. P. Bui, *Science*, 1998, **279**, 49.
- For a quick overview and recent findings on the HO_x chemistry in the upper troposphere see *IGAC Newsletter*, Issue no. 19, at <http://web.mit.edu/igac/www/>
- H. B. Singh, D. O'Hara, D. Herlth, W. Sachse, D. R. Blake, J. D. Bradshaw, M. Kanakidou and P. J. Crutzen, *J. Geophys. Res.*, 1994, **99**, 1805.
- T. Gierczak, J. B. Burkholder, S. Bauerle and A. R. Ravishankara, *Chem. Phys.*, 1998, **231**, 229.
- M. Wollenhaupt, S. A. Carl, A. Horowitz and J. N. Crowley, *J. Phys. Chem. A*, 2000, **104**, 2695.

- 8 W. B. DeMore, S. P. Sander, D. M. Golden, M. J. Molina, R. F. Hampson, M. J. Kurylo, C. J. Howard, C. E. Kolb and A. R. Ravishankara, *Chemical Kinetics and Photochemical Data for Use in Stratospheric Modeling*, NASA-JPL Publication 97-4, Jet Propulsion Laboratory, Pasadena, CA, 1997.
- 9 R. Atkinson, D. L. Baulch, R. A. Cox, R. F. Hampson, Jr., J. A. Kerr, M. J. Rossi and J. Troe, *J. Phys. Chem. Ref. Data*, 1999, **28**, 191.
- 10 S. Le Calvé, D. Hitier, G. Le Bras and A. Mellouki, *J. Phys. Chem. A*, 1998, **102**, 4579.
- 11 M. Wollenhaupt and J. N. Crowley, *J. Phys. Chem. A*, 2000, **104**, 6429.
- 12 T. Gierczak and A. R. Ravishankara, 16th International Symposium on Gas Kinetics, Cambridge, July 23–27, 2000, Poster PB 13.
- 13 G. Vasvári, I. Szilágyi, Á. Bencsura, K. Imrik, E. Farkas, S. Dóbe, T. Bérces, E. Henon, S. Canneaux and F. Bohr, *Phys. Chem. Chem. Phys.*, in preparation.
- 14 G. H. Dieke and H. M. Crosswhite, *J. Quant. Spectrosc. Radiat. Transfer*, 1962, **2**, 97.
- 15 N. Washida, S. Inomata and M. Furubayashi, *J. Phys. Chem. A*, 1998, **102**, 7924.
- 16 S. Dóbe, T. Bérces, F. Temps, H. Gg. Wagner and H. Ziemer, *25th Symp. (Int.) Combust. [Proc.]*, 1994, 775.
- 17 M. J. Frisch, G. W. Trucks, H. B. Schegel, P. M. W. Gill, B. G. Johnson, M. A. Robb, J. R. Cheeseman, T. A. Keith, G. A. Petersson, J. A. Montgomery, K. Raghavachari, M. A. Al-Laham, V. G. Zakrzewski, J. V. Ortiz, J. B. Foresman, J. Cioslowski, B. B. Stefanov, A. Nanayakkara, M. Challacombe, C. Y. Peng, P. Y. Ayala, W. Chen, M. W. Wong, J. L. Andres, E. S. Replogle, R. Gomperts, R. L. Martin, D. J. Fox, J. S. Binkley, D. J. Defrees, J. Baker, J. P. Stewart, M. Head-Gordon, C. Gonzalez, and J. A. Pople, *Gaussian 94*, Gaussian Inc., Pittsburgh, PA, 1995.
- 18 C. Møller and M. S. Plesset, *Phys. Rev.*, 1934, **46**, 618.
- 19 C. Gonzalez and H. B. Schlegel, *J. Chem. Phys.*, 1989, **90**, 2154.
- 20 R. J. Bartlett, *J. Phys. Chem.*, 1989, **93**, 1697.
- 21 S. Aloisio and J. S. Francisco, *J. Phys. Chem.*, 2000, **104**, 3211.
- 22 J. T. Jodkowski, M. T. Rayez, J. C. Rayez, T. Bérces and S. Dóbe, *J. Phys. Chem. A*, 1998, **102**, 9219; J. T. Jodkowski, M. T. Rayez, J. C. Rayez, T. Bérces and S. Dóbe, *J. Phys. Chem. A*, 1998, **102**, 9230.
- 23 D. T. Anderson, R. L. Schwartz, M. W. Todd and M. I. Lester, *Chem. Phys.*, 1998, **109**, 3461; M. D. Wheeler, M. Tsiouris, M. I. Lester and Gy. Lendvay, *J. Chem. Phys.*, 2000, **112**, 6590.
- 24 J. M. Bofill, S. Olivella, A. Sole and J. M. Anglada, *J. Am. Chem. Soc.*, 1999, **121**, 1337.
- 25 C. Oehlers, H. Gg. Wagner, H. Ziemer, F. Temps and S. Dóbe, *J. Phys. Chem. A*, 2000, **104**, 10511.
- 26 M. R. Soto and M. Page, *J. Phys. Chem.*, 1990, **94**, 3242.
- 27 P. H. Taylor, M. S. Rahman, M. Arif, B. Dellinger and P. Marshall, *26th Symp. (Int.) Combust. [Proc.]*, 1996, 497.